WALAILAK JOURNAL
http://wjst.wu.ac.th Mathematics

Radiation Effects on an Unsteady MHD Convective Flow Past a Semi-Infinite Vertical Permeable Moving Plate Embedded in a Porous Medium with Viscous Dissipation

Murali GUNDAGANI[1,*], Sivaiah SHERI[2], Ajit PAUL[1] and Marpadaga Chenna Krishna REDDY[3]

[1]*Department of Mathematics, SHIATS University, Allahabad, India*
[2]*Department of Mathematics, GITAM University, Hyderabad, India*
[3]*Department of Mathematics, Osmania University, Hyderabad, India*

(**[*]Corresponding author's e-mail: muraligundagani@yahoo.in**)

Received: 24 May 2012, Revised: 6 December 2012, Accepted: 5 April 2013

Abstract

The work presents an analysis of unsteady, two-dimensional, laminar, boundary-layer flow of a viscous, incompressible, electrically conducting and radiating fluid along a semi-infinite vertical permeable moving plate. Heat and mass transfer is analyzed by taking into account the effect of viscous dissipation. The dimensionless governing equations for this investigation are solved numerically by a finite element method. The effects of the various parameters on the velocity, temperature and concentration profiles are presented graphically and values of skin-friction, Nusselt number and Sherwood number for various values of physical parameters are presented in tables.

Keywords: MHD, radiation, porous medium, viscous dissipation, finite element method

Introduction

Simultaneous heat and mass transfer from different geometries embedded in porous media has many engineering and geophysical applications such as geothermal reservoirs, drying of porous solids, thermal insulation, and enhanced oil recovery, packed-bed catalytic reactors, cooling of nuclear reactors and underground energy transport. Bejan and Khair [1] treated one of the most fundamental cases, namely buoyancy- induced heat and mass transfer from a vertical plate embedded in a saturated porous medium. Cheng and Minkowycz [2] presented similarity solutions for free convection from a vertical plate in a fluid saturated porous medium. Lai and Kulacki [3] investigated coupled heat and mass transfer by mixed convection from an isothermal vertical plate in a porous medium.

There has been a renewed interest in studying magnetohydrodynamic (MHD) flow and heat transfer in porous and non-porous media due to the effect of magnetic fields on the boundary layer flow control and on the performance of many systems using electrically conducting fluids. Raptis *et al.* [4] analyzed hydromagnetic free convection flow through a porous medium between two parallel plates. Gribben [5] presented the boundary layer flow over a semi-infinite plate with an aligned magnetic field in the presence of a pressure gradient. He obtained solutions for large and small magnetic Prandtl number using the method of matched asymptotic expansion. Helmy [6] presented an unsteady two-dimensional laminar free convection flow of an incompressible, electrically conducting (Newtonian or polar) fluid through a porous medium bounded by infinite vertical plane surface of constant temperature. Gregantopoulos *et al.* [7] studied two-dimensional unsteady free convection and mass transfer flow of an incompressible viscous dissipative and electrically conducting fluid past an infinite vertical porous plate. For some industrial applications such as glass production and furnace design, and in space technology applications such as cosmical flight aerodynamics rocket, propulsion systems, plasma physics and spacecraft re-entry aerothermodynamics which operate at higher temperatures, radiation effects can be significant. Chambre and Young [8] have presented a first order chemical reaction in the neighborhood of a horizontal plate. Dekha *et al.* [9] investigated the effect of the first order homogeneous chemical reaction on the process of an unsteady flow past a vertical plate with a constant heat and mass transfer. Muthucumaraswamy [10] presented heat and mass transfer effects on a continuously moving isothermal vertical surface with uniform suction by taking into account the homogeneous first order chemical reaction. Muthucumaraswamy and Meenakshisundaram [11] investigated the theoretical study of chemical reaction effects on vertical oscillating plate with variable temperature and mass diffusion.

In all these investigations, the viscous dissipation is neglected. The viscous dissipation heat in the natural convective flow is important, when the flow field is of extreme size or at low temperature or in a high gravitational field. Gebhar [12] showed the importance of viscous dissipative heat in free convection flow in the case of isothermal and constant heat flux in the plate. Soundalgekar [13] analyzed the effect of viscous dissipative heat on the two dimensional unsteady, free convective flow past a vertical porous plate when the temperature oscillates in time and there is constant suction at the plate. Cookey *et al.* [14] investigated the influence of viscous dissipation and radiation on unsteady MHD free convection flow past an infinite heated vertical plate in porous medium with time dependent suction.

The role of thermal radiation on the flow and heat transfer process is of major importance in the design of many advanced energy conversion systems operating at higher temperatures. Thermal radiation within these systems is usually the result of emission by hot walls and the working fluid. Bakier and Gorla [15] studied thermal radiation effects on mixed convection from horizontal surfaces in porous medium. Bakier [16] reported the effect of radiation on the mixed convection flow on an isothermal vertical surface in a saturated porous medium and has obtained a self- similar solution. Hossain and Takhar [17] analyzed the effect of radiation on mixed convection along a vertical plate with uniform surface temperature. Kim and Fedorov [18] analyzed transient mixed radiative convective flow of a micropolar fluid past a moving semi-infinite vertical porous plate. Radiation effects on an unsteady MHD convective heat and mass transfer flow past a semi-infinite vertical permeable moving plate embedded in a porous medium was studied by Prasad and Reddy [19].

The objective of the present paper is to analyze the radiation effects on an unsteady two-dimensional laminar mixed convective boundary layer flow of a viscous, incompressible, electrically conducting fluid, along a vertical moving semi-infinite permeable plate with suction, embedded in a uniform porous medium, in the presence of a transverse magnetic field, by taking into account the effects of viscous dissipation. The dimensionless governing equations for this investigation are solved numerically by a finite element method. The behaviors of the velocity, temperature, concentration, skin-friction, Nusselt number and Sherwood number have been discussed for variations in the governing parameters.

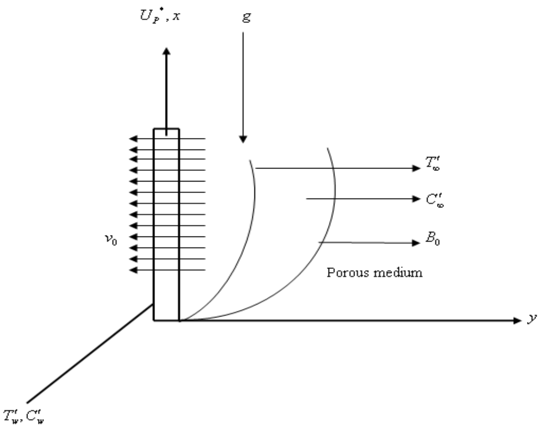

Figure 1 Physical model and coordinate system of the problem.

Formulation of the problem

An unsteady two-dimensional free convection flow of a viscous incompressible electrically conducting, and radiating fluid in an optically thick fluid past a semi-infinite vertical permeable moving plate embedded in a uniform porous medium, in the presence of a transverse magnetic field, by taking into account the effects of viscous dissipation considered (**Figure 1**). The x'- axis is taken along the plate in the upward direction and the y' - axis is taken normal to the plate. A uniform magnetic field is applied in the direction perpendicular to the plate. The fluid is assumed to be slightly conducting, and hence the magnetic Reynolds number is much less than unity and the induced magnetic field is negligible in comparison with the applied magnetic field. The foreign mass present in the flow is assumed to be at low level and hence Soret and Dufour effects are negligible. Further, due to the semi-infinite plane surface assumption, the flow variables are functions of normal distance y' and the time t' only. Now, under the usual Boussinesq's approximation, the governing boundary layer equations of the problem are;

$$\frac{\partial v'}{\partial y'} = 0 \tag{1}$$

$$\frac{\partial u'}{\partial t'} + v'\frac{\partial u'}{\partial y'} = -\frac{1}{\rho}\frac{\partial p'}{\partial x'} + v\frac{\partial^2 u'}{\partial y'^2} + g\beta(T' - T'_\infty) + g\beta^*(C' - C'_\infty) - \frac{v\,u'}{K'} - \frac{\sigma B_0^2 u'}{\rho} \tag{2}$$

$$\frac{\partial T'}{\partial t'} + v'\frac{\partial T'}{\partial y} = \frac{k}{\rho\, c_p}\left[\frac{\partial^2 T'}{\partial y'^2} - \frac{1}{k}\frac{\partial q'}{\partial y'}\right] + \frac{v}{c_p}\left(\frac{\partial u'}{\partial y'}\right)^2 \tag{3}$$

$$\frac{\partial^2 q'}{\partial y'^2} - 3\alpha^2 q' - 16\sigma^*\alpha T_\infty'^3\frac{\partial T}{\partial y'} = 0 \tag{4}$$

$$\frac{\partial C'}{\partial t'} + v'\frac{\partial C'}{\partial y'} = D\frac{\partial^2 C'}{\partial y'^2} - K'_r C' \tag{5}$$

where u', v' are the velocity components in the x', y' directions, respectively. t' - the time, ρ -the fluid density, p' - the pressure, ν - the kinematic viscosity, σ - fluid electrical conductivity, c_s - concentration susceptibility, c_p - the specific heat at constant pressure, g - the acceleration due to gravity, β and β^* - the thermal and concentration expansion coefficient respectively, B_0 - the magnetic induction, α - the fluid thermal diffusivity, K' - the permeability of the porous medium, T' - temperature of the fluid in the boundary layer, C' - species concentration in the boundary layer, k -the thermal conductivity, q' - the radiative heat flux, σ^* - the Stefan-Boltzmann constant, D - the mass diffusivity, K'_r - the chemical reaction parameter. The third and fourth terms on the right hand side of the momentum Eq. (2) denote the thermal and concentration buoyancy effects, respectively. Also, the second and third terms on the right hand side of the energy Eq. (3) and represent the radiative heat flux and viscous dissipation, respectively.

It is assumed that the permeable plate moves with a constant velocity in the direction of the fluid flow and the free stream velocity follows the exponentially increasing small perturbation law. In addition, it is assumed that the temperature and concentration at the wall as well as the suction velocity are exponentially varying with time. Eq. (4) is the differential approximation for radiation under fairly broad realistic assumptions.

The boundary conditions for the velocity, temperature and concentration fields are;

$$\begin{aligned} & u' = u'_p, \quad T' = T'_\infty + \varepsilon(T'_w - T'_\infty)e^{n't'}, \\ & C' = C'_\infty + \varepsilon(C'_w - C'_\infty)e^{n't'} \qquad at \;\; y' = 0 \\ & u' = U'_\infty = U_0 + \varepsilon\left(1 + \varepsilon e^{n't'}\right), \\ & T' \to T'_\infty, \quad C' \to C'_\infty \qquad as \;\; y' \to \infty \end{aligned} \tag{6}$$

where u'_p is the plate velocity, T'_w and C'_w are the wall dimensional temperature and concentration, respectively, T'_∞ and C'_∞ are the free stream dimensional temperature and concentration, respectively, U'_∞ the free stream velocity, U_0 and n' -the constant. From the Eq. (1), it is clear that suction velocity normal to the plate is either a constant or a function of time. Hence, it is assumed in the form;

$$v' = -V_0\left(1 + \varepsilon\, A e^{n't'}\right) \tag{7}$$

where A is a real positive constant, ε and $\varepsilon\, A$ are small values less than unity and V_0 is a scale of suction velocity which is a non-zero positive constant. Outside the boundary layer, Eq. (2) gives;

$$-\frac{1}{\rho}\frac{\partial p'}{\partial x'} = \frac{dU'_\infty}{dt'} + \frac{\nu U'_\infty}{K'} + \frac{\sigma B_0'^{} U'_\infty}{\rho} \tag{8}$$

Since the medium is optically thin with relatively low density and $\alpha << 1$, the radiative heat flux given by Eq. (3), in the spirit of Cogley *et al.* [20] becomes;

$$\frac{\partial q'}{\partial y'} = 4\alpha^2\left(T' - T'_\infty\right) \tag{9}$$

where $\alpha^2 = \int_0^\infty \delta\lambda \frac{\partial B}{\partial T'}$, and B is the Planck's function.

In order to write the governing equations and the boundary conditions in dimensionless form, the following non-dimensional quantities are introduced.

$$\begin{aligned} & u = \frac{u'}{U_0},\; v = \frac{v'}{V_0},\; y = \frac{V_0 y'}{\nu},\; U_p = \frac{u'_p}{U_0}, \\ & U_\infty = \frac{U'_\infty}{U_0},\; n = \frac{n'\nu}{V_0^2},\;\; t = \frac{t' V_0^2}{\nu}, \\ & \theta = \frac{T' - T'_\infty}{T'_w - T'_\infty},\;\; C = \frac{C' - C'_\infty}{C'_w - C'_\infty}, \end{aligned}$$

$$K = \frac{K' V_0^2}{\nu^2}, \ \Pr = \frac{\nu \rho C_p}{k} = \frac{\nu}{\alpha},$$
$$Sc = \frac{\nu}{D}, \ M = \frac{\sigma B_0^2 \nu}{\rho V_0^2}, \ R^2 = \frac{\alpha^2 (T'_w - T'_\infty)}{\rho c_p k U_0^2},$$
$$Ec = \frac{U_0^2}{c_p (T'_w - T'_\infty)}$$
$$Gr = \frac{\nu \beta g (T'_w - T'_\infty)}{U_0 V_0^2}, \ Gm = \frac{\nu \beta^* g (C'_w - C'_\infty)}{U_0 V_0^2}, \tag{10}$$
$$K_r = \frac{K'_r \nu}{V_0^2}$$

In view of Eqs. (4) and (7 - 10), Eqs. (2), (3) and (5) reduce to the following dimensionless form;

$$\frac{\partial u}{\partial t} - (1 + \varepsilon A e^{nt}) \frac{\partial u}{\partial y} = \frac{dU_\infty}{dt} + \frac{\partial^2 u}{\partial y^2} + Gr\theta + GmC + N(U_\infty - u) \tag{11}$$

$$\frac{\partial \theta}{\partial t} - (1 + \varepsilon A e^{nt}) \frac{\partial \theta}{\partial y} = \frac{1}{\Pr}\left[\frac{\partial^2 \theta}{\partial y^2} - R^2\right] + Ec\left(\frac{\partial u}{\partial y}\right)^2 \tag{12}$$

$$\frac{\partial C}{\partial t} - (1 + \varepsilon A e^{nt}) \frac{\partial C}{\partial y} = \frac{1}{Sc}\frac{\partial^2 C}{\partial y^2} - K_r C \tag{13}$$

where $N = \left(M + \frac{1}{K}\right)$ and $Gr, Gm, M, K,$ $\Pr, R, Ec,$ Sc and K_r are the thermal Grashof number, solutal Grashof number, magnetic field parameter, permeability parameter, Prandtl number, radiation parameter, Eckert number, Schmidt number and chemical reaction parameter, respectively.

The corresponding boundary conditions are;

$$\begin{aligned} &u = U_p, \ \theta = 1 + \varepsilon e^{nt}, \ C = 1 + \varepsilon e^{nt} && at \ y = 0 \\ &u \to U_\infty = 1 + \varepsilon e^{nt}, \ \theta \to 0, \ C \to 0 && as \ y \to \infty \end{aligned} \tag{14}$$

Solution of the problem

By applying the Galerkin finite element method for Eq. (11) over the element (e), $(y_j \le y \le y_k)$ is;

$$\int_{y_j}^{y_k} N^{(e)T}\left[\frac{\partial^2 u^{(e)}}{\partial y^2} + P\frac{\partial u^{(e)}}{\partial y} - \frac{\partial u^{(e)}}{\partial t} - N_1 u^{(e)} + R_1\right] dy = 0 \tag{15}$$

where

$P = 1 + A\varepsilon e^{nt}$, $R_1 = n\varepsilon e^{nt} + Gr\theta + GmC + N_1 U_\infty$,
$N_1 = \left(M + \frac{1}{K} \right)$

Integrating the first term in equation by parts one obtains;

$$N^{(e)^T} \left. \frac{\partial u^{(e)}}{\partial y} \right\}_{y_j}^{y_k} - \int_{y_j}^{y_k} \begin{cases} \frac{\partial N^{(e)^T}}{\partial y} \frac{\partial u^{(e)}}{\partial y} - \\ N^{(e)^T} \left(P \frac{\partial u^{(e)}}{\partial y} + \frac{\partial u^{(e)}}{\partial t} + N_1 u^{(e)} - R_1 \right) \end{cases} dy = 0 \tag{16}$$

Neglecting the first term in Eq. (16) we get;

$$\int_{y_j}^{y_k} \left\{ \begin{array}{l} \frac{\partial N^{(e)^T}}{\partial y} \frac{\partial u^{(e)}}{\partial y} - N^{(e)^T} \\ \left(P \frac{\partial u^{(e)}}{\partial y} - \frac{\partial u^{(e)}}{\partial t} - N_1 u^{(e)} + R_1 \right) \end{array} \right\} dy = 0$$

Let $u^{(e)} = N^{(e)} \phi^{(e)}$ be the linear piecewise approximation solution over the element (e), $(y_j \le y \le y_k)$ where $N^{(e)} = [N_j \quad N_k]$, $\phi^{(e)} = [u_j \quad u_k]^T$ and $N_j = \frac{y_k - y}{y_k - y_j}$, $N_k = \frac{y - y_j}{y_k - y_j}$ are the basis functions. One obtains;

$$\int_{y_j}^{y_k} \left\{ \begin{bmatrix} N_j' N_j' & N_j' N_k' \\ N_j' N_k' & N_k' N_k' \end{bmatrix} \begin{bmatrix} u_j \\ u_k \end{bmatrix} \right\} dy - P \int_{y_j}^{y_k} \left\{ \begin{bmatrix} N_j N_j' & N_j N_k' \\ N_j' N_k & N_k' N_k \end{bmatrix} \begin{bmatrix} u_j \\ u_k \end{bmatrix} \right\} dy + \int_{y_j}^{y_k} \left\{ \begin{bmatrix} N_j N_j & N_j N_k \\ N_j N_k & N_k N_k \end{bmatrix} \begin{bmatrix} \dot{u}_j \\ \dot{u}_k \end{bmatrix} \right\} dy + N_1 \int_{y_j}^{y_k} \left\{ \begin{bmatrix} N_j N_j & N_j N_k \\ N_j N_k & N_k N_k \end{bmatrix} \begin{bmatrix} u_j \\ u_k \end{bmatrix} \right\} dy = R_1 \int_{y_j}^{y_k} \begin{bmatrix} N_j \\ N_k \end{bmatrix} dy$$

Simplifying we get;

$$\frac{1}{l^{(e)^2}} \begin{bmatrix} 1 & -1 \\ -1 & 1 \end{bmatrix} \begin{bmatrix} u_j \\ u_k \end{bmatrix} - \frac{P}{2l^{(e)}} \begin{bmatrix} -1 & 1 \\ -1 & 1 \end{bmatrix} \begin{bmatrix} u_j \\ u_k \end{bmatrix} + \frac{1}{6} \begin{bmatrix} 2 & 1 \\ 1 & 2 \end{bmatrix} \begin{bmatrix} u_j^\bullet \\ u_k^\bullet \end{bmatrix} + \frac{N_1}{6} \begin{bmatrix} 2 & 1 \\ 1 & 2 \end{bmatrix} \begin{bmatrix} u_j \\ u_k \end{bmatrix} = \frac{R_1}{2} \begin{bmatrix} 1 \\ 1 \end{bmatrix}$$

where prime and dot denote differentiation w.r.t y and time t, respectively. Assembling the element equations for two consecutive elements $y_{i-1} \le y \le y_i$ and $y_i \le y \le y_{i+1}$ the following is obtained;

$$\frac{1}{l^{(e)2}}\begin{bmatrix}1 & -1 & 0\\ -1 & 2 & -1\\ 0 & -1 & 1\end{bmatrix}\begin{bmatrix}u_{i-1}\\ u_i\\ u_{i+1}\end{bmatrix}-\frac{P}{2l^{(e)}}\begin{bmatrix}-1 & 1 & 0\\ -1 & 0 & 1\\ 0 & -1 & 1\end{bmatrix}\begin{bmatrix}u_{i-1}\\ u_i\\ u_{i+1}\end{bmatrix}$$
$$+\frac{1}{6}\begin{bmatrix}2 & 1 & 0\\ 1 & 4 & 1\\ 0 & 1 & 2\end{bmatrix}\begin{bmatrix}\dot{u}_{i-1}\\ \dot{u}_i\\ \dot{u}_{i+1}\end{bmatrix}+\frac{N_1}{6}\begin{bmatrix}2 & 1 & 0\\ 1 & 4 & 1\\ 0 & 1 & 2\end{bmatrix}\begin{bmatrix}u_{i-1}\\ u_i\\ u_{i+1}\end{bmatrix}=\frac{R_1}{2}\begin{bmatrix}1\\ 2\\ 1\end{bmatrix} \tag{17}$$

Now put row corresponding to the node i to zero, from Eq. (17) the difference schemes with $l^{(e)} = h$ is;

$$\frac{1}{h^2}\left[-u_{i-1}+2u_i-u_{i+1}\right]-\frac{P}{2h}\left[-u_{i-1}+u_{i+1}\right]$$
$$+\frac{1}{6}\left[\dot{u}_{i-1}+4\dot{u}_i+\dot{u}_{i+1}\right]+\frac{N_1}{6}\left[u_{i-1}+4u_i+u_{i+1}\right] = R_1$$

Applying the Crank-Nicholson method to the above equation we get;

$$A_1u_{i-1}^{j+1}+A_2u_i^{j+1}+A_3u_{i+1}^{j+1}= A_4u_{i-1}^{j}+A_5u_i^{j}+A_6u_{i+1}^{j}+R^* \tag{18}$$

Applying a similar procedure to Eqs. (12) and (13) we get;

$$B_1\theta_{i-1}^{j+1}+B_2\theta_i^{j+1}+B_3\theta_{i+1}^{j+1}= B_4\theta_{i-1}^{j}+B_5\theta_i^{j}+B_6\theta_{i+1}^{j}+R^{**} \tag{19}$$

$$C_1C_{i-1}^{j+1}+C_2C_i^{j+1}+C_3C_{i+1}^{j+1}= C_4C_{i-1}^{j}+C_5C_i^{j}+C_6C_{i+1}^{j} \tag{20}$$

where

$A_1 = 2-6r+3Phr+N_1k,$ $A_2 = 8+12r+4N_1k,$
$A_3 = 2-6r-3Phr+N_1k,$ $A_4 = 2+6r-3Phr-N_1k,$
$A_5 = 8-12r-4N_1k,$ $A_6 = 2+6r+3Phr-N_1k,$
$B_1 = 2\Pr-6r+3\Pr Phr+\Pr Rk,$ $B_2 = 8\Pr+12r+4\Pr Rk,$
$B_3 = 2\Pr-6r-3\Pr Phr+\Pr Rk,$ $B_4 = 2\Pr+6r-3\Pr Phr-\Pr Rk,$
$B_5 = 8\Pr-12r-4\Pr Rk,$ $B_6 = 2\Pr+6r+3\Pr Phr-\Pr Rk,$
$C_1 = 2Sc-6r+3PScrh+ScK_rk,$ $C_2 = 8Sc+12r+4ScK_rk,$
$C_3 = 2Sc-6r-3PScrh+ScK_rk,$ $C_4 = 2Sc+6r-3PScrh-ScK_rk,$
$C_5 = 8Sc-12r-4ScK_rk,$ $C_6 = 2Sc+6r+3PScrh-ScK_rk,$
$R^* = 12(Gr)k\theta_i^j+12(Gm)kC_i^j+12kN_1U_\infty+12kn\varepsilon e^{nt}$
$R^{**} = 12r\Pr Ec(u[i+1]-u[i])^2$

Here $r = \dfrac{k}{h^2}$ and $h,\ k$ are the mesh sizes along $y-$direction and time $t-$direction, respectively. Index i refers to the space and j refers to the time. In Eqs. (19) and (20), taking $i = 1(1)n$ and using initial and boundary conditions (14), the following system of equations are obtained.

$$A_i X_i = B_i \qquad i = 1(1)3 \tag{21}$$

where A_i's are matrices of order n and X_i, B_i's column matrices having $n-$components. The solutions of the above system of equations are obtained by using the Thomas algorithm for velocity, temperature and concentration. Also, numerical solutions for these equations are obtained by the C-program. In order to prove the convergence and stability of the finite element method, the same C-program was run with slightly changed values of h and k and no significant change was observed in the values of u, θ and *C*. Hence, the finite element method is stable and convergent.

The skin-friction, Nusselt number and Sherwood number are important physical parameters for this type of boundary layer flow.

The skin-friction at the plate, which in the non-dimensional form is given by;

$$C_f = \frac{\tau'_w}{\rho\, U_0 V_0} = \left(\frac{\partial u}{\partial y}\right)_{y=0} \tag{22}$$

The rate of heat transfer coefficient, which in the non-dimensional form in terms of the Nusselt number is given by;

$$Nu = -x\frac{\left(\dfrac{\partial T'}{\partial y'}\right)_{y'=0}}{T'_w - T'_\infty} \Rightarrow Nu\,\mathrm{Re}_x^{-1} = -\left(\frac{\partial \theta}{\partial y}\right)_{y=0} \tag{23}$$

The rate of the mass transfer coefficient, which in the non-dimensional form in terms of the Sherwood number, is given by;

$$Sh = -x\frac{\left(\dfrac{\partial C'}{\partial y'}\right)_{y'=0}}{C'_w - C'_\infty} \Rightarrow Sh\,\mathrm{Re}_x^{-1} = -\left(\frac{\partial C}{\partial y}\right)_{y=0} \tag{24}$$

where $\mathrm{Re}_x = \dfrac{V_0 x}{\nu}$ is the local Reynolds number.

Results and discussion

The formulation of the problem that accounts for the radiation effects on an unsteady MHD convective heat and mass transfer flow past a semi-infinite vertical permeable moving plate embedded in a porous medium with viscous dissipation has been performed in the preceding sections. The governing equations of the flow field were solved analytically, using the finite element method, and the expressions for the velocity, temperature, concentration, skin-friction, Nusselt and Sherwood numbers were obtained. In order to get a physical insight into the problem, the above physical quantities are computed numerically for different values of the governing parameters viz., thermal Grashof number Gr, solutal Grashof number Gm, magnetic parameter M, permeability parameter K, Prandtl number $\Pr$, radiation parameter R, Eckert number Ec, Schmidt number Sc, chemical reaction parameter K_r and the plate velocity U_p. In order to ascertain the accuracy of the numerical results, the present study is compared with the previous study. The velocity and temperature profiles are compared with the available solution of Prasad and Reddy [19] in **Figures 2** and **3**. It is observed that the present results are in good agreement with that of Prasad and Reddy [19].

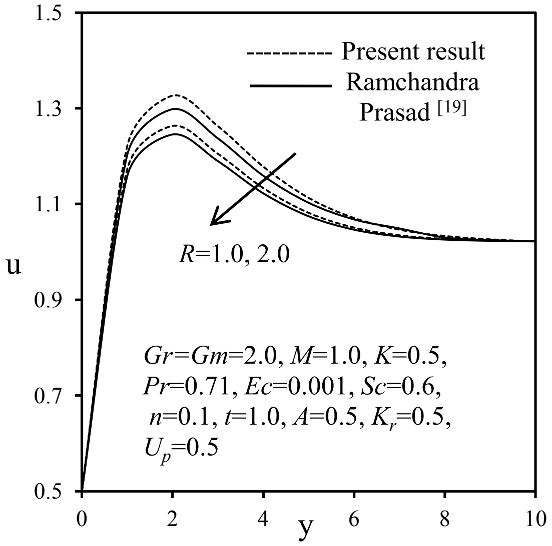

Figure 2 Comparison of the velocity profiles for different values of *R*.

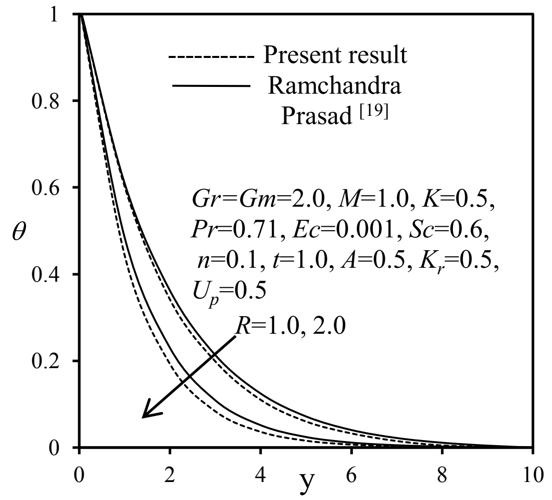

Figure 3 Comparison of the temperature profiles for different values of *R*.

For the case of different values of thermal Grashof number Gr, the velocity profiles in the boundary layer are shown in **Figure 4**. It is observed that an increase in Gr leads to decrease in the values of velocity due to enhancement in the buoyancy force. Here the positive values of Gr correspond to cooling of the surface.

In addition, the curve shows that the peak values of the velocity decrease rapidly near the wall of the porous plate as the Grashof number increases and then decays to the free stream velocity. **Figure 5** presents typical velocity profiles in the boundary layer for various values of the solutal Grashof number Gm, while all other parameters are kept at some fixed values. The velocity distribution attains a distinctive maximum value in the vicinity of the plate surface and then decreases properly to approach the free stream value. As expected, the fluid velocity increases and the peak value is more distinctive due to an increase in the concentration buoyancy effects represented by Gm. This is evident in the increase in the value of u as Gm increases in **Figure 5**. The effect of magnetic field on velocity profiles in the boundary layer is depicted in **Figure 6**. From this figure it is seen that the velocity starts from a minimum value at the surface and increases till it attains a peak value and then starts decreasing until it reaches a minimum value at the end of the boundary layer for all the values of the magnetic field parameter. It is interesting to note that the effect of the magnetic field is to decrease the value of the velocity profiles throughout the boundary layer. The effect of the magnetic field is more prominent at the point of peak value. The peak value drastically decreases with an increase in the value of magnetic field, because the presence of a magnetic field in an electrically conducting fluid introduce a force called the Lorentz force. This force acts against the flow if the magnetic field is applied in the normal direction, as in the present problem. This type of resisting force slows down the fluid velocity as shown in this figure. **Figure 7** shows the velocity profiles for different values of the permeability parameter *K*, clearly as *K* increases the peak values of the velocity tend to increase.

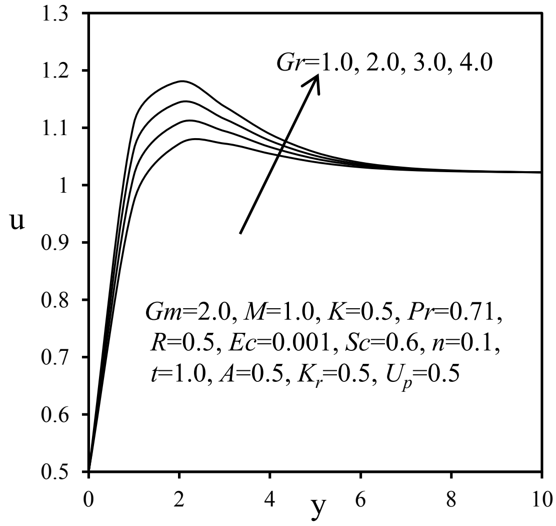

Figure 4 Effect of *Gr* on velocity.

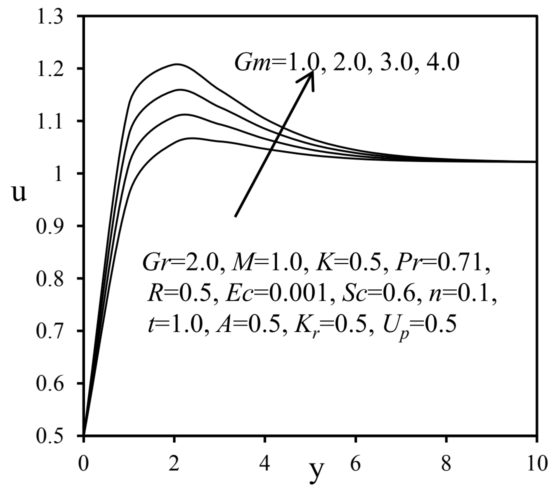

Figure 5 Effect of *Gm* on velocity.

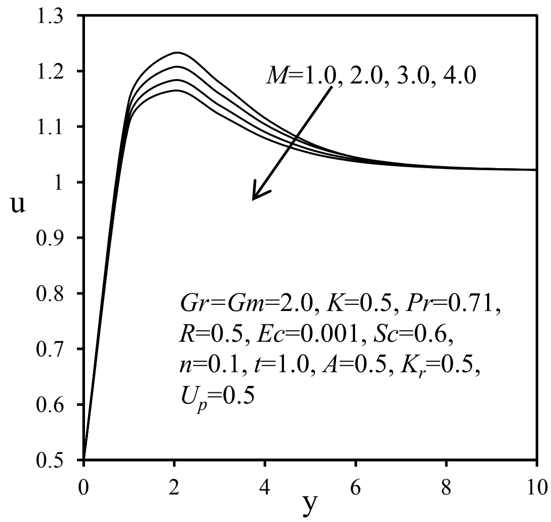

Figure 6 Effect of *M* on velocity.

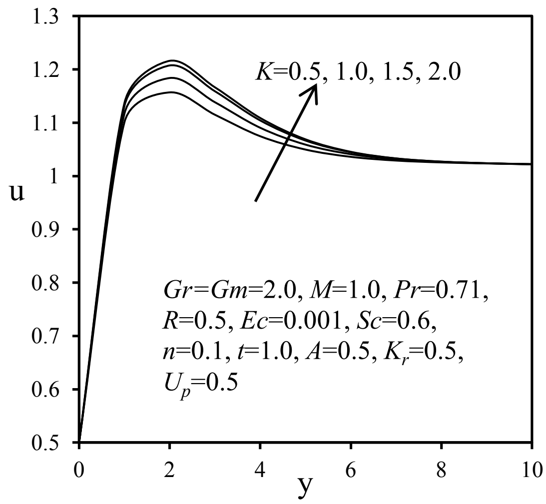

Figure 7 Effect of *K* on velocity.

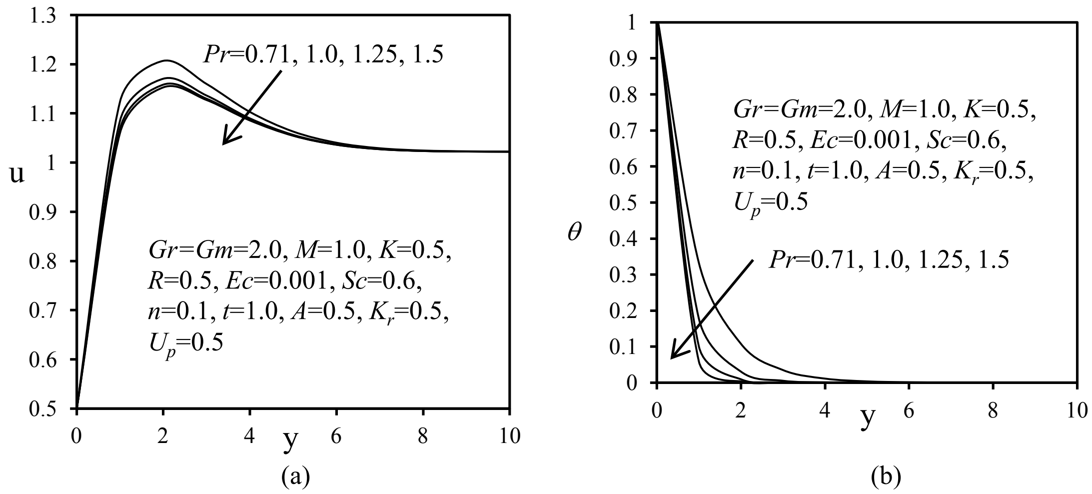

Figure 8 (a) Effect of *Pr* on velocity and (b) effect of *Pr* on temperature.

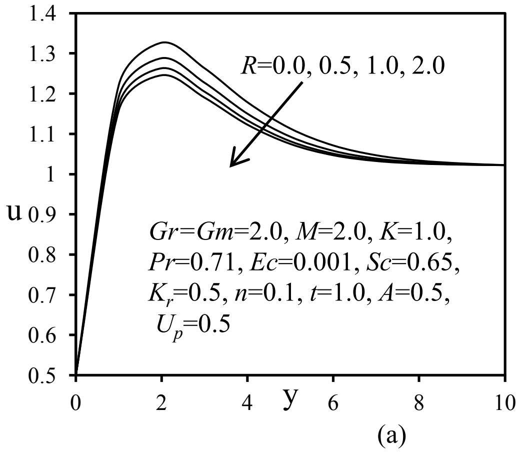

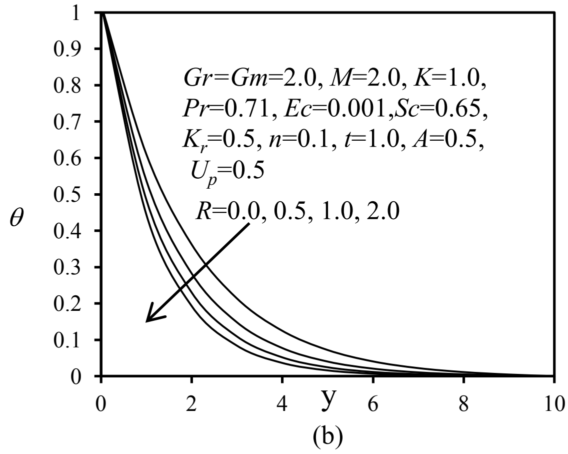

Figure 9 (a) Effect of *R* on velocity and (b) effect of *R* on temperature.

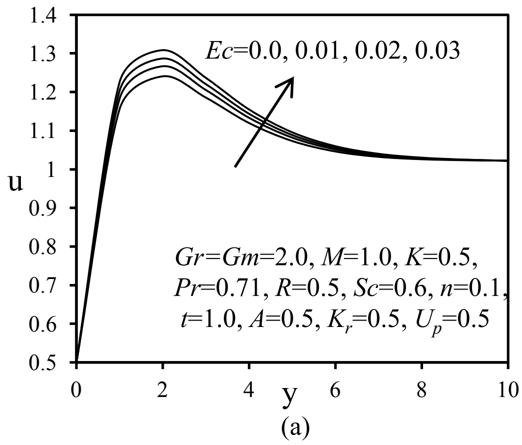

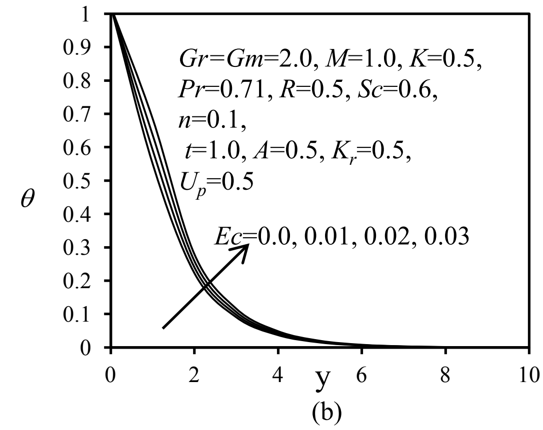

Figure 10 (a) Effect of *Ec* on velocity and (b) effect of *Ec* on temperature.

Figures 8(a)-8(b) illustrate the velocity and temperature profiles for different values of the Prandtl number, $\Pr$. The numerical results show that the effect of increasing values of the Prandtl number result in an increasing velocity. The numerical results show that an increase in the Prandtl number results in a decrease of the thermal boundary layer and in general lower average temperature within the boundary layer. The reason is that smaller values of $\Pr$ are equivalent to an increase in the thermal conductivity of the fluid and therefore heat is able to diffuse away from the heated surface more rapidly for higher values of $\Pr$. Hence in the case of smaller Prandtl number the thermal boundary layer is thicker and the rate of heat transfer is reduced. For different values of the radiation parameter *R*, the velocity and temperature profiles are plotted in **Figures 9(a)-9(b)**. It is obvious that an increase in the radiation parameter R results in a decrease in the velocity and temperature within the boundary layer, as well as a decrease in the thickness of the velocity and temperature of the boundary layer. The effect of the viscous dissipation parameter i.e. the Eckert number Ec on the velocity and temperature are shown in **Figures 10(a)-10(b)**. Greater viscous dissipative heat causes a rise in temperature as well as the velocity.

Figures 11(a)-11(b) display the effects of the Schmidt number Sc on the velocity and concentration profiles, respectively. As the Schmidt number increases the concentration decreases. This causes the concentration buoyancy effects to decrease yielding a reduction in the fluid velocity. The reductions and the velocity and concentration profiles are accompanied by simultaneous reductions in the velocity and concentration boundary layers. These behaviors are clearly shown in **Figures 11(a)-11(b). Figure 12(a)** shows the velocity distribution *u* against *y* for different values of K_r. We noticed that the velocity decreases with increases K_r. **Figure 1(b)** displays the effects of the chemical reaction K_r on concentration profiles *C*. We observe that concentration profile *C* decreases with an increase in K_r. **Figure 13** shows the velocity distribution across the boundary layer for several values of plate moving velocity U_p in the direction of the fluid flow. Although we have different initial plate moving velocities, the velocity decreases to a constant value for given material parameters.

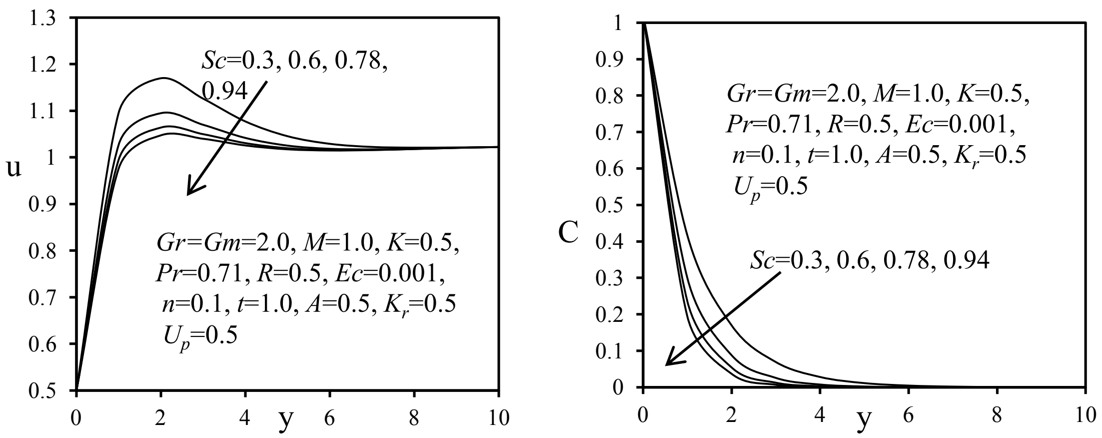

Figure 11 (a) Effect of *Sc* on velocity, (b) effect of *Sc* on concentration.

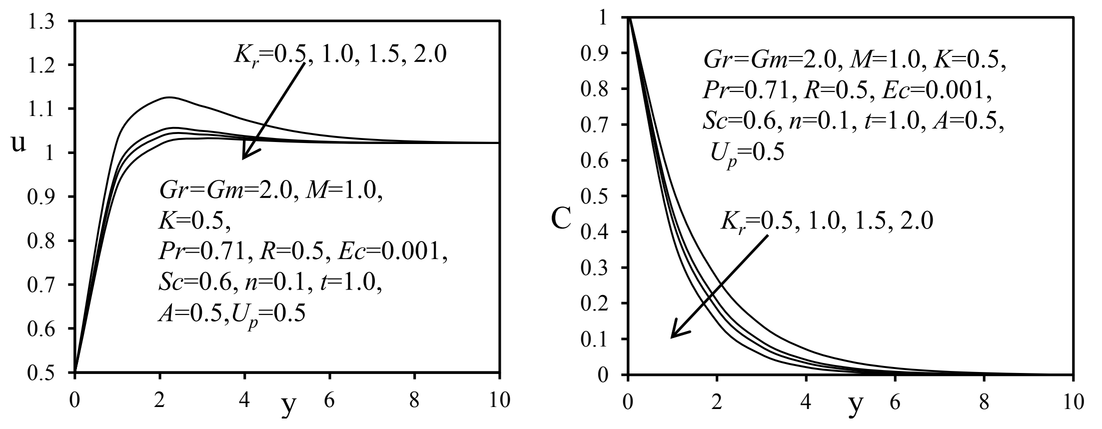

Figure 12 (a) Effect of K_r on velocity, (b) effect of K_r on concentration.

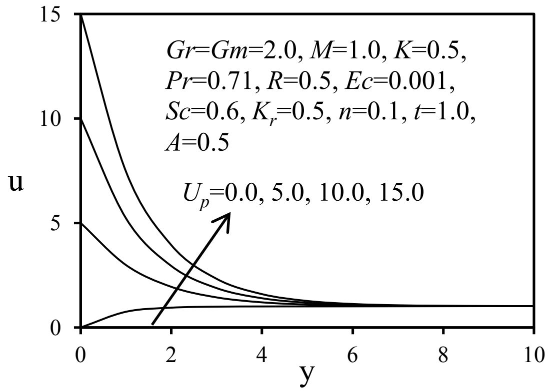

Fig 13 Effect of U_p on velocity.

Tables 1 - 5 present the effects of the thermal Grashof number, solutal Grashof number, radiation parameter, Schmidt number and Eckert number on the skin-friction C_f Nusselt number Nu and Sherwood number Sh. From **Tables 1** and **2**, it is observed that as Gr or Gm increases, the skin-friction coefficient increases. However, from **Table 3**, it can be seen that as the radiation parameter increases, the skin-friction decreases and the Nusselt number increases. From **Table 4**, it is noticed that an increase in the Schmidt number reduces the skin-friction and increases the Sherwood number. Finally, it is observed from **Table 5** that as the Eckert number increases the skin-friction increases, and the Nusselt number decreases.

Table 1 Effects Gm of on C_f (Reference values as in **Figure 5**).

Gm	C_f
0.0	1.9732
1.0	2.5114
2.0	3.0508
3.0	3.5907
4.0	4.1321

Table 2 Effects of Gr on C_f (Reference values as in **Figure 4**).

Gr	C_f
0.0	1.6858
1.0	2.0965
2.0	2.5116
3.0	2.09337
4.0	3.03649

Table 3 Effects of R on C_f and $Nu\,\mathrm{Re}_x^{-1}$ (Reference values as in **Figures 9(a)-9(b)**).

R	C_f	$Nu\,\mathrm{Re}_x^{-1}$
0.0	2.6868	0.6812
0.5	2.5120	1.1179
1.0	2.4321	1.3847
2.0	2.3471	1.7586

Table 4 Effects of Sc on C_f and $Sh\,\mathrm{Re}_x^{-1}$ (Reference values as in **Figures 11(a)-11(b)**).

Sc	C_f	$Sh\,\mathrm{Re}_x^{-1}$
0.30	2.6075	0.3001
0.60	2.5116	0.6008
0.78	2.4664	0.7807
0.94	2.4331	0.9412

Table 5 Effects of Ec on C_f and $Nu\,\mathrm{Re}_x^{-1}$ (Reference values as in **Figures 10(a)-10(b)**).

Ec	C_f	$Nu\,\mathrm{Re}_x^{-1}$
0.0	2.5054	1.1486
0.01	2.5690	0.8562
0.02	2.6318	0.5634
0.03	2.6952	0.2710

Conclusions

The governing equations for unsteady MHD convective heat and mass transfer flow fast a semi-infinite vertical permeable moving plate embedded in a porous medium with radiation was formulated. Viscous dissipation effects were also included in the present work. The plate velocity is maintained at a constant value and the flow was subjected to a transverse magnetic field. The dimensionless governing equations are solved numerically by a finite element method. Numerical evaluations of the closed form results were performed and graphical results were obtained to illustrate the details of the flow and heat and mass transfer characteristics and their dependence on some physical parameters. It was found that when thermal and solutal Grashof numbers were increased, the thermal and concentration buoyancy effects were enhanced and thus, the fluid velocity increased. However, the presence of radiation effects caused reductions in fluid temperature, which resulted in a decrease in fluid velocity. Also, when the Schmidt number was increased, the concentration level was decreased resulting in a decrease in fluid velocity. The velocity as well as concentration decreases with an increase in the chemical reaction parameter. In addition, it was found that the skin friction coefficient increased due to an increase in thermal and concentration buoyancy effects while it decreased due to an increase in either radiation parameter or the Schmidt number. However, the Nusselt number increased as the radiation parameter increased and the Sherwood number also increased as the Schmidt number increased. An increase in the Eckert number leads to an increase in the skin-friction and a decrease in the Nusselt number.

References

[1] A Bejan and KR Khair. Heat and mass transfer by natural convection in the porous medium. *Int. J. Heat Mass Tran*. 1985; **28**, 909-18.

[2] P Cheng and WK Minkowycz. Free convection about a vertical plate embedded in porous medium with application to heat transfer from a dike. *J. Geophys. Res*. 1977; **82**, 2040-4.

[3] FC Lai and FA Kulacki. Coupled heat and mass transfer by natural convection from vertical surfaces in a porous medium. *Int. J. Heat Mass Tran.* 1991; **34**, 1189-94.

[4] A Raptis, A Massalas and G Tzivanidis. Hydromagnetic free convection flow through a porous medium between two parallel plates. *Phys. Lett.* 1982; **90a**, 288-9.

[5] RJ Gribben. The magnetohydrodynamic boundary layer in the presence of a pressure gradient. *Proc. Royal. Soc. London* 1965; **287**, 123-41.

[6] KA Helmy. MHD unsteady free convection flow past a vertical porous plate. *ZAMM.* 1998; **78**, 255-70.

[7] GA Gregantopoulos, J Koullias, CL Goudas and C Courogenis. Free convection and mass transfer effects on the hydromagnetic oscillatory flow past an infinite vertical porous plate. *Astrophys. Space Sci.* 1981; **74**, 357-89.

[8] PL Chambre and JD Young. On the diffusion of a chemically reactive species in a laminar boundary layer flow. *Phys. Fluids Flow* 1958; **1**, 48-54.

[9] R Dekha, UN Das and VM Soundalgekar. Effects on mass transfer on flow past an impulsively started infinite vertical plate with constant heat flux and chemical reaction. *Forschung im Ingenieurwesen* 1994; **60**, 284-309.

[10] R Muthucumaraswamy. Effects of a chemical reaction on a moving isothermal surface with suction. *Acta Mech.* 2002; **155**, 65-72.

[11] R Muthucumaraswamy and S Meenakshisundaram. Theoretical study of chemical reaction effects on vertical oscillating plate with variable temperature. *Theor. Appl. Mech.* 2006; **33**, 245-57.

[12] B Gebhar. Effects of viscous dissipative in natural convection. *J. Fluid Mech.* 1962; **14**, 225-32.

[13] VM Soundalgekar. Viscous dissipative effects on unsteady free convective flow past an vertical porous plate with constant suction. *Int. J. Heat Mass Tran.* 1972; **15**, 1253-61.

[14] C Israel-Cookey, A Ogulu and VB Omubo-Pepple. Influence of viscous dissipation on unsteady MHD free convection flow past an infinite heated vertical plate in porous medium with time dependent suction. *Int. J. Heat Mass Tran.* 2003; **46**, 2305-11.

[15] AY Bakier and RSR Gorla. Thermal radiation effects on horizontal surfaces in saturated porous medium. *Transport Porous Media* 1996; **23**, 357-61.

[16] AY Bakier. Thermal radiation effect on mixed convection from vertical surface in saturated porous medium. *Int. Comm. Heat Mass Tran.* 2001; **28**, 119-26.

[17] MA Hossain and HS Takhar. Radiation effect on mixed convection along a vertical plate with uniform surface temperature. *Heat Mass Tran.* 1996; **31**, 243-8.

[18] YJ Kim and AG Fedorov. Transient mixed radiative convection flow of a micro polar fluid past a moving semi-infinite vertical porous plate. *Int. J. Heat Mass Tran.* 2003; **46**, 1751-8.

[19] VR Prasad and NB Reddy. Radiation effects on an unsteady MHD convective heat and mass transfer flow past a semi-infinite vertical permeable moving plate embedded in a porous medium. *J. Energ. Heat Mass Tran.* 2008; **30**, 57-68.

[20] AC Cogley, WG Vincenti and SE Gilles. Differential approximation to radiative heat transfer in a non-grey gas near equilibrium. *AIAA. J.* 1968; **6**, 551-3.